Dyes and Pigments **18** (1992) 237–249

The Distribution Diagram and the Visible Spectra of *o*-Methyl Red Species in Aqueous Solutions

Khalid M. Tawarah

Department of Chemistry, Yarmouk University, Irbid, Jordan

(Received 25 June 1991; accepted 8 October 1991)

ABSTRACT

The distribution diagram of the diprotic, the monoprotic and the anion forms of o-*methyl red is given in water at 25°C. The monoprotic form has a maximum fraction of 0·894 at pH 3·6. The calculated visible spectrum of the monoprotic form was found to be pH-dependent. The spectrum calculated at pH 3·6 is consistent with other* o-*methyl red spectra which describe two overlapping equilibria where the monoprotic form behaves either as a conjugate acid or as a conjugate base. The first- and second-derivative spectra are reported and correlated with the absorption spectrum at pH 5·37. The position of the maximum absorption of the diprotic form or of the monoprotic form is red-shifted by about 100 nm from that of the anion or the triprotic form.*

1 INTRODUCTION

o-Methyl red, *o*-(*p*-dimethylaminophenylazo)-benzoic acid, has been the subject of several investigations concerning its photochromism,[1] resonance Raman spectra,[2] inclusion complexes with cyclodextrins,[3] pK determination,[4–7] structure[8] and the effect of pH and temperature on its absorption spectra.[9] In addition, *o*-methyl red has been selected as an example for testing the matrix-rank method[10] in the analysis of the absorption spectra of multicomponent systems and for evaluating a graphical method for determining the number of species in solution from spectrophotometric data.[11]

The object of this present work is to establish the distribution diagram of the anion form, the monoprotic form and the diprotic form (see Fig. 1) of *o*-methyl red in aqueous solutions at 25°C in the pH range 0 to 9 by using

Dyes and Pigments 0143-7208/92/$05.00

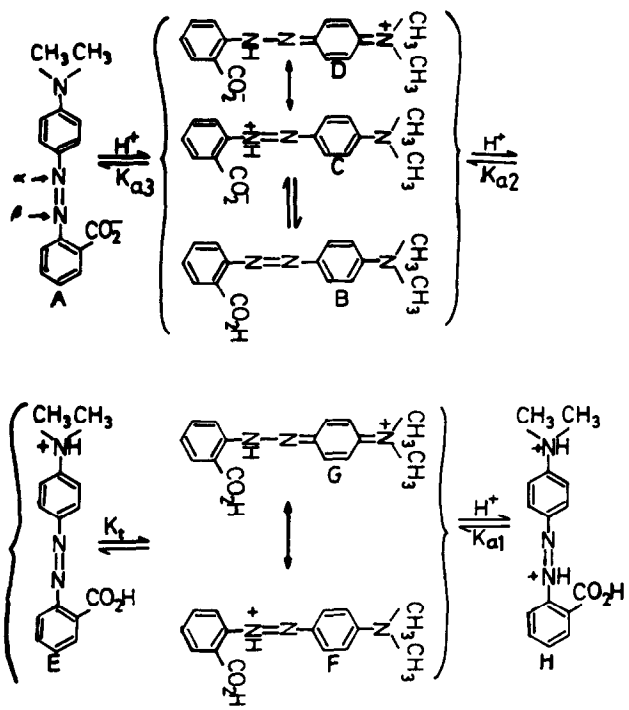

Fig. 1. The acid-base equilibria of *o*-methyl red in aqueous solutions.

the recently reported[7] thermodynamic values of Ka_2 and Ka_3. An attempt is also made to report the calculated absorption spectrum of the monoprotic form of *o*-methyl red in the wavelength range 350 to 600 nm, as well as the first- and the second-derivative spectra of a solution of *o*-methyl red which contains only the anion and the monoprotic form. The correlation of the derivative spectra with the absorption spectrum of *o*-methyl red at pH 5·37 is discussed. The visible spectra pertaining to two acid-base equilibria (equilibria designated by Ka_2 and Ka_3 in Fig. 1) are reported and compared with previous spectra.[7]

2 EXPERIMENTAL

The acid form of *o*-methyl red ($C_{15}H_{15}N_3O_2$) was purchased from Sigma (St Louis, Missouri, USA) and was subjected to a methanol Soxhlet extraction until a constant melting point was achieved at 181°C (melting point of the untreated sample was 179°C). The test sample was dried at 90°C for 16 h before use. The details of the experimental procedures pertaining to the preparation of the stock solution of *o*-methyl red, the calibration of the pH

meter, and the description of the instruments used in this study has been given previously.[7] The visible spectra were recorded at $25{\cdot}0 \pm 0{\cdot}1$°C over the wavelength range 350–600 nm. The spectra were machine-digitized with a digital sampling interval of 5 nm. The absorbance data obtained at every 5 nm (51 absorbance readings) were converted into molar absorptivity data and were plotted on linear graph paper. No spectroscopic features were missed in the sampling interval as indicated by the chart recorder.

3 RESULTS AND DISCUSSION

Three acid-base equilibria are shown in Fig. 1, with acid dissociation constants Ka_1, Ka_2 and Ka_3. The structures given in Fig. 1 are based on previous discussions.[7,8] Two of these equilibria (those of Ka_2 and Ka_3) were considered overlapping[5,7] in view of the relative magnitudes of Ka_2 and Ka_3 compared with that of Ka_1. Therefore only the distribution of the species participating in these overlapping equilibria are considered in this study. These species are the anion form (structure A in Fig. 1), the monoprotic form (structure B and the resonance hybrid of the zwitterionic structures C and D in Fig. 1), and the diprotic form (the tautomeric mixture of structure E and the resonance hybrid of structures G and F in Fig. 1). By considering the thermodynamic expressions of Ka_2 and Ka_3, it can be shown that the fractions, F_i, of the species participating in the overlapping equilibria are given as follows:

$$F_{MR^-} = Ka_2Ka_3/D \tag{1}$$

$$F_{HMR} = Ka_2[H^+]f_{H^+}(f_{MR^-}/f_{HMR})/D \tag{2}$$

$$F_{H_2MR^+} = [H^+]^2f_{H^+}^2(f_{MR^-}/f_{H_2MR^+})/D \tag{3}$$

where the denominator, (D) is defined by eqn (4):

$$D = Ka_2Ka_3 + Ka_2[H^+]f_{H^+}(f_{MR^-}/f_{HMR}) + [H^+]^2f_{H^+}^2(f_{MR^-}/f_{H_2MR^+}) \tag{4}$$

The symbol f_i represents the activity coefficient of the indicated species, while MR^-, HMR, and H_2MR^+ stand for the anion form, the monoprotic form and the diprotic form, respectively.

The calculations of the fractions defined by eqns (1)–(3) were based on the following considerations.

(a) The contribution of *o*-methyl red to the ionic strength, I, was neglected since its concentration is of the order 10^{-5} mol dm^{-3}.

(b) The ionic strength was calculated from the pH of the solution, $I = 10^{-pH}$ where the use of HCl or NaOH was assumed for adjusting the pH of the solution.

(c) The activity coefficient of the neutral monoprotic form, f_{HMR}, was assumed to be unity in the pH range 0–9.

(d) The activity coefficients f_{MR^-} and $f_{H_2MR^+}$ of the singly charged ions were assumed equal.

(e) The product $[H^+]f_{H^+}$, which is the activity of the H^+ species, a_{H^+}, was calculated from the pH of the solution, $a_{H^+} = 10^{-pH}$.

(f) In the pH range $0 \leq pH \leq 2$ the activity coefficient $f_{H_2MR^+}$ was calculated according to eqn (5):

$$\log f_{H_2MR^+} = -(0{\cdot}51\sqrt{I})(1 + \sqrt{I})^{-1} + 0{\cdot}20I \qquad (5)$$

which is the Guggenheim extension of the Debye–Huckel equation for singly charged organic ions in water at 25°C.[12]

(g) For pH values higher than 2, the activity coefficients f_{MR^-} and $f_{H_2MR^+}$ were calculated according to the Debye–Huckel limiting law: $\log f_i = -0{\cdot}51\sqrt{I}$.

(h) The thermodynamic values of Ka_2 and Ka_3 in water at 25°C were taken from Ref. 7 with $Ka_2 = 4{\cdot}16 \times 10^{-3}$ and $Ka_3 = 1{\cdot}40 \times 10^{-5}$ mol dm^{-3}.

(i) The contribution of the triprotic form (structure H in Fig. 1) to the total concentration of *o*-methyl red was neglected in the pH range 0–9, since Ka_1 of *o*-methyl red is expected to be much larger than Ka_2 or Ka_3 and that of Ka_1 is $1{\cdot}22 \times 10^6$ mol dm^{-3} for methyl orange[13] and $2{\cdot}51 \times 10^4$ mol dm^{-3} for methyl yellow.[14]

The fractions given by eqns (1)–(3) were calculated at 35 pH values in the pH range 0–9 and the results are plotted in Fig. 2. This figure indicates that the fraction of the monprotic form (curve B in Fig. 2) is always less than unity at any pH value. The maximum fraction of the monoprotic form corresponds to a pH value of 3·6. At this pH the distribution curve of the monoprotic form appears symmetrical about the vertical line at pH 3·6. The fractions of the anion and the diprotic forms are nearly equal at pH 3·6 which is the isoelectric point of *o*-methyl red.[5] The fractions obtained at pH 3·6 are 0·051 for the anion form, 0·894 for the monoprotic form and 0·055 for the diprotic form. It was found that *o*-methyl red is entirely in the anion form at pH values > 7 and in the diprotic form at pH 0·5. It was also found that the diprotic–monoprotic equilibrium is the dominating one in the pH range $0 < pH < 3$ (i.e., the fraction of the anion is nil), while the monoprotic–anion equilibrium is the only equilibrium in the pH range $4{\cdot}5 \leq pH \leq 7$ (i.e., the fraction of the diprotic form is nil).

According to the matrix-rank method, Wallace & Katz[10] have concluded that in the pH range 2–7 at least three absorbing species were present in *o*-methyl red solutions and a fourth species was suspected. The same conclusion was reached by Coleman *et al.*[11] who applied a graphical method to the same data. According to Figs 1 and 2, it is proposed that the three

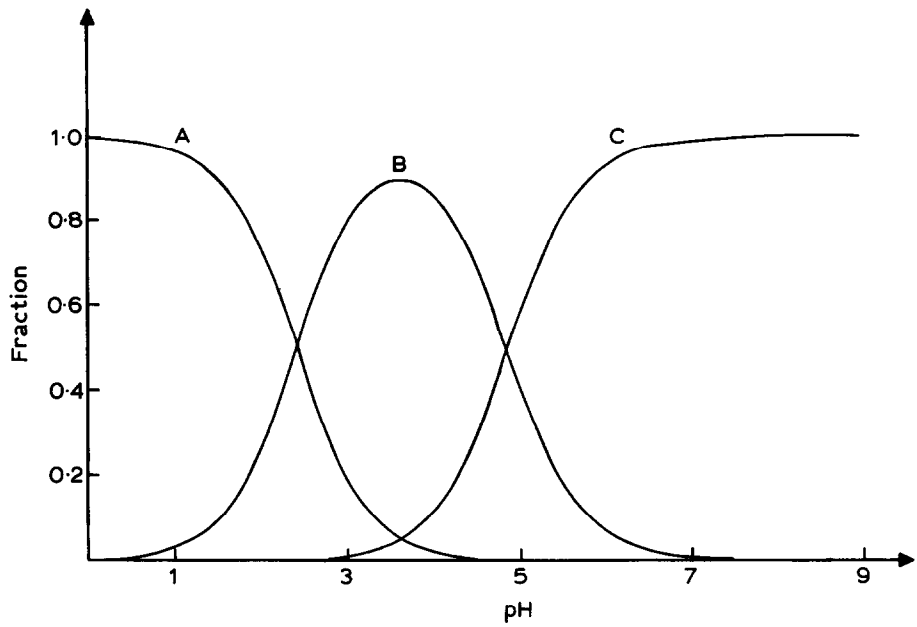

Fig. 2. The distribution diagram of *o*-methyl red species in water at 25°C. The letters A, B and C stand for the diprotic form, the monoprotic form and the anion form, respectively.

confirmed absorbing species are the anion form (structure A in Fig. 1), the resonance hybrid of the zwitterionic structures (structures C and D in Fig. 1) and the azonium tautomer of the diprotic form (the resonance hybrid of structures G and F in Fig. 1), while the suspected fourth species is the nonionic structure (structure B in Fig. 1) of the monoprotic form, whose abundance is expected to be very low.[7,8] Structure E in Fig. 1, which is the ammonium tautomer of the diprotic form, is excluded since it does not absorb appreciably in the visible region.[7] Structure H in Fig. 1 is also excluded since it does not exist in dilute acidic solutions of *o*-methyl red. The distribution curves shown in Fig. 2 suggest that a reasonable test of the matrix-rank method[10] or the graphical method[11] can be carried out in two separate ranges of pH. The first range, $0 < pH < 3$, excludes the anion form and the determined number of the absorbing species can be discussed by considering one acid-base equilibrium which involves the diprotic and the monoprotic forms of *o*-methyl red. The second range, $4{\cdot}5 < pH < 7$, excludes the diprotic form and the determined number of the absorbing species can be discussed by considering one acid-base equilibrium which involves the monoprotic and the anion forms of *o*-methyl red. A distribution diagram for the species indicated in Fig. 2 has been reported[15] but with the omission of the activity coefficients and the use of a different value of Ka_3.

Three *o*-methyl red solutions were required in order to calculate the visible spectrum of the monoprotic form of *o*-methyl red at a given pH. In 0·32 mol dm^{-3} aqueous HCl (pH 0·5) *o*-methyl red exists entirely in the diprotic form. The visible spectrum of $9{\cdot}285 \times 10^{-6}$ mol dm^{-3} of *o*-methyl red in 0·32 mol dm^{-3} aqueous HCl is given in Fig. 3 (curve 1) and was considered to represent the spectrum of the diprotic form. Curve 2 in Fig. 3 represents the spectrum of the anion form at pH 9·5 with a concentration of $1{\cdot}857 \times 10^{-5}$ mol dm^{-3}. The absorbances of a $9{\cdot}285 \times 10^{-6}$ mol dm^{-3} of *o*-methyl red solution at pH 3·6 were measured at 51 wavelengths in the wavelength range 350–600 nm. According to Fig. 2, the visible spectrum of *o*-methyl red at pH 3·6 can be considered as a composite spectrum to which the anion form, the monoprotic form and the diprotic form contribute. The molar

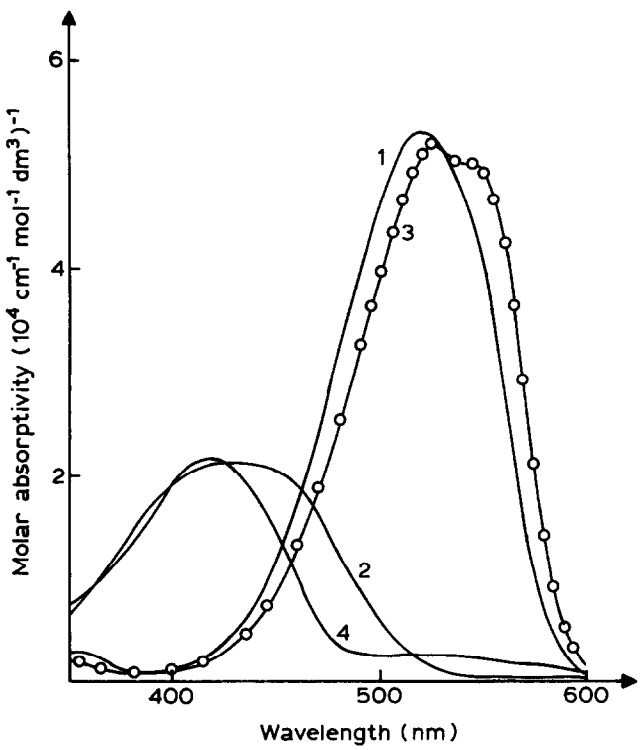

Fig. 3. The visible spectra of the several forms of *o*-methyl red at 25°C. The sequence 1–4 stands for the diprotic form ($9{\cdot}285 \times 10^{-6}$ mol dm^{-3} *o*-methyl red in 0·32 mol dm^{-3} aqueous HCl), the anion form ($1{\cdot}857 \times 10^{-5}$ mol dm^{-3} *o*-methyl red at pH 9·5), the monoprotic form (calculated at pH 3·6 from the spectrum of $9{\cdot}285 \times 10^{-6}$ mol dm^{-3} *o*-methyl red), and the triprotic form ($1{\cdot}857 \times 10^{-5}$ mol dm^{-3} *o*-methyl red in aqueous 90 wt% H_2SO_4), respectively.

absorptivities of these forms are related to the apparent molar absorptivity of *o*-methyl red by the following equation:

$$\varepsilon_{app} = (F_{H_2MR^+})(\varepsilon_{H_2MR^+}) + (F_{HMR})(\varepsilon_{HMR}) + (F_{MR^-})(\varepsilon_{MR^-}) \quad (6)$$

where $\varepsilon_{app.}$ is the apparent molar absorptivity of the mixture and can be calculated at any wavelength by knowing the total concentration and the absorbances of *o*-methyl red at the desired pH, $\varepsilon_{H_2MR^+}$ is the molar absorptivity of the diprotic form and can be obtained at pH 0·5 as given in curve 1 of Fig. 3, ε_{MR^-} stands for the molar absorptivity of the anion form and can be obtained in alkaline solutions as given in curve 2 of Fig. 3, and ε_{HMR} represents the molar absorptivity of the monoprotic form which can be calculated at any wavelength by using eqn (6) since all the other quantities appearing in this equation are known at a given pH. The molar absorptivities of the monoprotic form were calculated at 51 wavelengths according to eqn (6) at pH 3·6 and the resulting spectrum of the monoprotic form is given in Fig. 3 (curve 3).

Figure 3 indicates that the molar absorptivities of the monoprotic and diprotic forms of *o*-methyl red are equal in the wavelength range 380–400 nm and the sequence of the spectra remains the same outside this region (down to 350 nm or up to 527 nm). The spectra of the monoprotic and the diprotic forms bisect at 527 nm. In order to elucidate that the intersection point at 527 nm is an authentic isosbestic point, the spectra of two other solutions of *o*-methyl red are shown in Fig. 4 (curve 2 at pH 2·42 and curve 3 at pH 2·00) together with the spectra of the monoprotic and the diprotic forms. These spectra have a common crossing point at 527 nm indicating that the isosbestic point represents an apparently two-species equilibrium, viz:

$$H_2MR^+ \overset{Ka_2}{\rightleftharpoons} H^+ + HMR \quad (7)$$

Our results concerning the spectra of the monoprotic and the diprotic forms of *o*-methyl red, as given in Fig. 3, are not in agreement with the previously reported results of Ramette *et al.*[5] By examining the spectra reported by Ramette *et al.*,[5] it was found that the spectra of the monoprotic and the diprotic forms bisect twice at about 426 nm and 508 nm and the maximum molar absorptivity of the monoprotic form is higher than that of the diprotic form. It should be pointed out, however, that Ramette *et al.*[5] used ethanolic stock solutions, while only water was used in this present study. Other discrepancies with the work of Ramette *et al.*[5] have been previously noted.[7] Another observation that can be deduced from Fig. 3 is that the spectra of the monoprotic and the anion forms bisect once at 467 nm. Figure 5 shows the calculated spectrum of the monoprotic form and the spectrum of the anion form, together with the spectra of two *o*-methyl

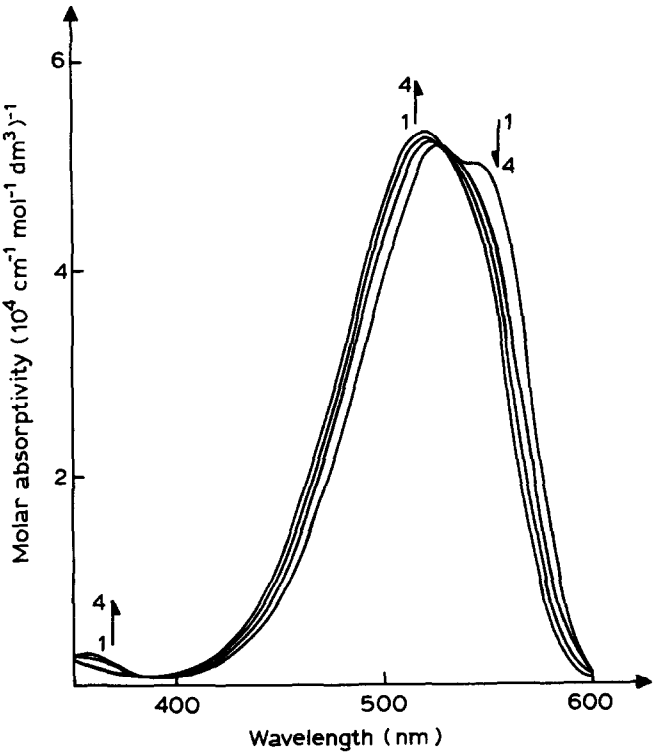

Fig. 4. The visible spectra that describe the diprotic–monoprotic equilibrium of *o*-methyl red at 25°C. The sequence 1–4 stands for the monoprotic form calculated at pH 3·6, *o*-methyl red at pH 2·42, *o*-methyl red at pH 2·00 and the diprotic form, respectively.

red solutions obtained at pH 4·9 and at pH 5·37. These spectra have a common crossing point at 467 nm, which is in agreement with other reports.[7,9] This isosbestic point represents the following acid-base equilibrium

$$HMR \overset{Ka_3}{\rightleftharpoons} H^+ + MR^- \tag{8}$$

A characteristic feature of the calculated spectrum of the monoprotic form is the appearance of two peaks at about 525 and 547 nm as can be seen on curve 3 of Fig. 3. By comparing the spectra of Figs 4 and 5 (see spectra 2 and 3 in both figures), it can be concluded that the appearance of two peaks in the visible region is more noticeable in *o*-methyl red solutions at high pH values which favour the establishment of the equilibrium given by eqn (8). Spectra similar to those of Fig. 5, which show the two-peak feature have been previously reported.[7,9] The disappearance of the two-peak feature at low pH and its appearance at high pH values has led to the conclusion that the structure of the monoprotic form is pH-dependent. Therefore structures

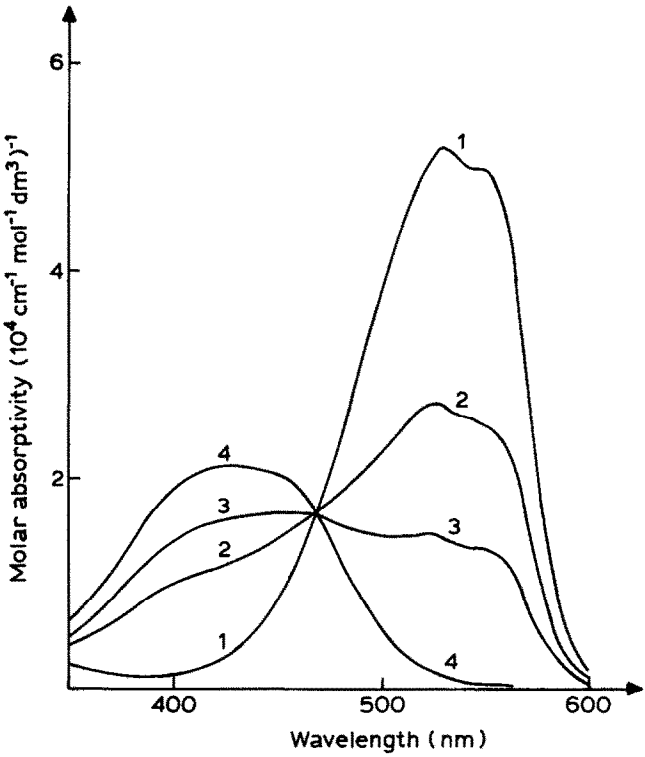

Fig. 5. Visible spectra illustrating the monoprotic–anion equilibrium of *o*-methyl red at 25°C. The sequence 1–4 stands for the monoprotic form calculated at pH 3·6, *o*-methyl red at pH 4·91, *o*-methyl red at pH 5·37 and the anion form, respectively.

other than those given in Fig. 1 can be considered for the monoprotic form. Two structures can be proposed. The first structure involves an intramolecular hydrogen bonding between the —COOH group and the *β*-nitrogen of the azo linkage, while the second structure can be obtained by having the proton of the monoprotic form attached to the nitrogen of the dimethyl amino group. This structure is a tautomer for the resonance hybrid of structures C and D in Fig. 1. The effect of pH on the relative abundance of any one of the possible structures of the monoprotic form is predicted to affect the calculated spectrum. This prediction was substantiated by calculating the spectrum of the monoprotic form at pH 4·91 and 5·37. Figure 6 shows three calculated spectra for the monoprotic form obtained at pH values of 3·6, 4·91 and 5·37. The fraction of the diprotic form is nil at pH 4·91 and 5·37. The spectra of Fig. 6 cross at about 480 nm and show appreciable differences in molar absorptivities in the wavelength region of maximum absorption. However, the two-peak feature is evident in Fig. 6 and the wavelength corresponding to each peak is pH-independent. An obvious

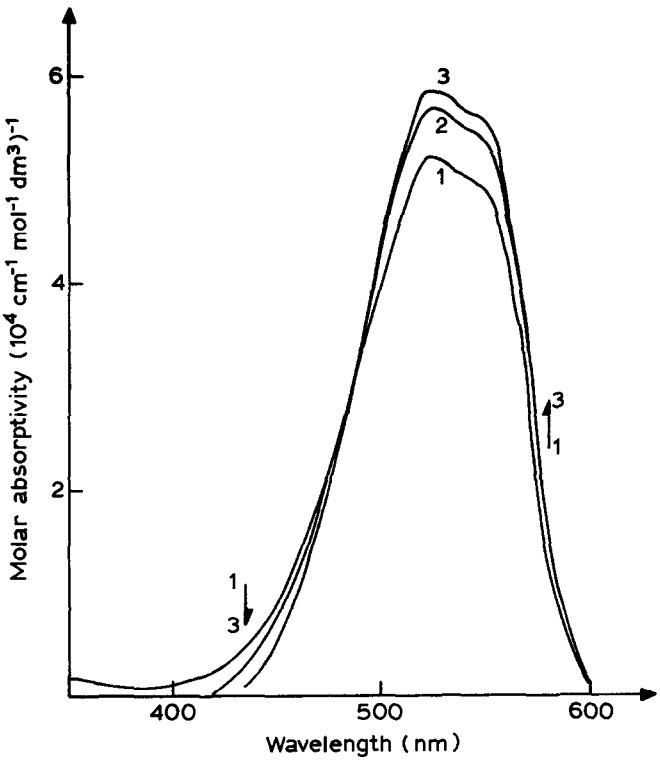

Fig. 6. Effect of pH on the calculated visible spectrum of the monoprotic form of *o*-methyl red at 25°C. The sequence 1–3 stands for spectra calculated at pH values of 3·6, 4·91 and 5·37, respectively.

conclusion to be drawn from Fig. 6 is that the assignment of a unique structure for the monoprotic form is improbable. The lack of isosbestic points at 467 and 527 nm in Fig. 6 has led to the conclusion that only the monoprotic structures prevailing at pH 3·6 can satisfy the coexistence of the two acid-base equilibria given by eqns (7) and (8) and can give isosbestic points at 527 and 467 nm as indicated in Figs 4 and 5, respectively.

Curve A in Fig. 7 represents the visible spectrum of *o*-methyl red solution at pH 5·37, while the curves designated as B and C are the first- and the second-derivative spectra of the same solution in the wavelength range 350–600 nm. By ignoring the spikes at about 390 nm on curve A of Fig. 6 (which are due to instrument noise) and considering the wavelength range 400–550 nm, the points a, b, c and d on the absorption spectrum can be correlated with those on the derivative spectra. Point a occurs at 448 nm and the first derivative of the spectrum is zero at this wavelength, while the second derivative significantly changes its sign. Since the anion of *o*-methyl

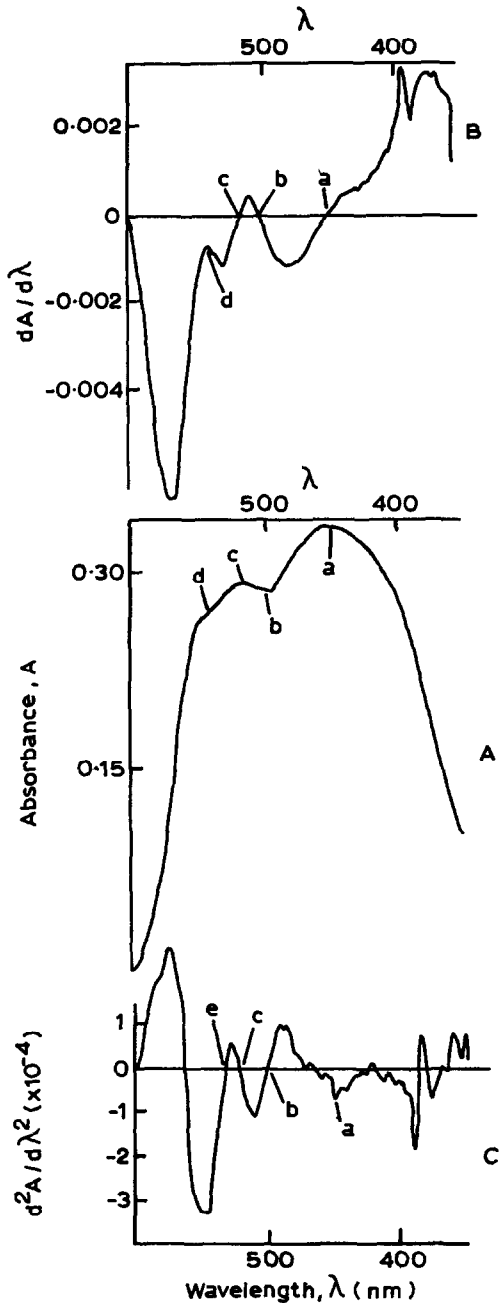

Fig. 7. The absorption and derivative spectra of $1{\cdot}857 \times 10^{-5}$ mol dm^{-3} *o*-methyl red at pH 5·37 and 25°C. The letters A, B and C represent the absorption spectrum, the first-derivative spectrum and the second-derivative spectrum, respectively. The significance of the letters a, b, c, d and e is given in the text.

red absorbs appreciably at 448 nm (see curve 2 in Fig. 3), the maximum occurring at 448 nm on curve A is mainly due to the anion form where its fraction is 0·77 at pH 5·37. Point b occurs at 500 nm and appears as a local minimum on the absorption spectrum. Both the first derivative and the second derivative are zero at this wavelength. Point c occurs at 517 nm and appears as a local maximum on curve A. The first derivative and the second derivative are both zero at this point. Point d occurs at 540 nm on the absorption spectrum and seems to be an inflection point. However, at 540 nm the first derivative is not zero (point d on spectrum B) but changes its sign significantly at 540 nm, while the second derivative is zero at 532 nm (point e on curve C). Since the anion form does not absorb significantly beyond 500 nm (see curve 2 in Fig. 3), the features at 517 nm and at about 540 nm on curve A can be attributed to the monoprotic form. The absorption occurring at 517 nm on curve A of Fig. 7 is blue-shifted by comparison with the maximum occurring at 525 nm on the spectrum of the monoprotic form given in Fig. 6. However, the peak occurring at 547 nm in Fig. 6 is evident on curve A of Fig. 7 but its location by the derivative spectra is not evident.

The visible spectrum of *o*-methyl red in aqueous 90 wt% H_2SO_4 is shown in Fig. 3. At this high acidity the color of *o*-methyl red solution is yellow. However, addition of NaOH solution to a diluted portion of the H_2SO_4/*o*-methyl red solution changed the color from yellow to red then to yellow at high pH. This observation is in agreement with a previous conclusion[7] concerning the colors of the macroscopic forms of *o*-methyl red. Structure H in Fig. 1, which is a tripotic form, is proposed to account for curve 4 in Fig. 3.

Before commenting on the spectra of Fig. 3, it should be pointed out that the electronic transitions of the azobenzene derivatives that occur in the visible region involve the molecular orbitals of the nitrogens of the azo linkage.[16] The lowest energy transition in azobenzene is an $n \rightarrow \pi^*$ transition, while the lowest energy transition in the protonated azobenzene is a $\pi \rightarrow \pi^*$ transition.[16] This implies that the addition of a proton to the azo linkage results in a change in the ground state of the electronic transition in the azobenzene system. The maximum absorption of azobenzene occurs at 320 nm in 95% ethanol while the maximum absorption of the protonated azobenzene occurs at 430 nm in 95% H_2SO_4.[14] Figure 3 indicates that the position of the maximum absorption of the monoprotic or the diprotic forms of *o*-methyl red is red-shifted by about 100 nm compared with that of the anion or the triprotic form. Also the maximum molar absorptivity of the monoprotic or the diprotic form is about two times greater than that of the anion or the triprotic form. Since several tautomeric and resonance structures can be written for the monoprotic and the diprotic forms compared with the case of the anion or the triprotic form, the occurrence of

the electronic transition of the monoprotic or the diprotic form at lower energies is probably a consequence of this fact.

ACKNOWLEDGEMENT

The author thanks Mr Sa'ib J. Khouri for his assistance in the absorbance measurements.

REFERENCES

1. Lovrien, R., Pesheck, P. & Tisel, W., *J. Am. Chem. Soc.*, **96** (1974) 244.
2. Machida, K., Kim, B., Saito, Y., Igarashi, K. & Uno, T., *Bull. Chem. Soc. Jpn*, **47** (1974) 78.
3. Buvari, A. & Barcza, L., *J. Incl. Phenom.*, **7** (1989) 313.
4. Reilley, C. N. & Smith, E. M., *Anal. Chem.*, **32** (1960) 1233.
5. Ramette, R. W., Dartz, E. A. & Kelly, P. W., *J. Phys. Chem.*, **66** (1962) 527.
6. Valentini, L., Gianazza, E. & Righetti, P. G., *J. Biochem. Biophys. Methods*, **3** (1980) 323.
7. Tawarah, K. M. & Abu-Shamleh, H. M., *Dyes and Pigments*, **17** (1991) 203.
8. Williams, I. W., *Shc. Sci. Rev.*, **49** (1968) 410.
9. Griffiths, T. R. & Potts, P. J., *Analytica Chimica Acta.*, **71** (1974) 1.
10. Wallace, R. M. & Katz, S. M., *J. Phys. Chem.*, **68** (1964) 3890.
11. Coleman, J. S., Varga, L. P. & Mastin, S. H., *Inorg. Chem.*, **9** (1970) 1015.
12. Rochester, C. H., *Acidity Functions.* Academic Press, London, 1970, p. 7.
13. Reeves, R. L., *J. Am. Chem. Soc.*, **88** (1966) 2240.
14. Sawicki, E., *J. Org. Chem.*, **22** (1957) 365.
15. Abu-Shamleh, H. M., MSc thesis, Yarmouk University, 1990.
16. Schenk, G. H., *Absorption of Light and Ultraviolet Radiation: Fluorescence and Phosphoresence Emission.* Allyn & Bacon, Boston, 1973, p. 234.